Textile & Leather Review

ISSN 2623-6281| www.tlr-journal.com | 10.31881/TLR

Degradation Characteristics of PBDEs in Flame-Retardant Textiles in Response to the EU POPs Regulation

Fangzheng Yuan, Hong Zhang

How to cite: Yuan F, Zhang H. Degradation Characteristics of PBDEs in Flame-Retardant Textiles in Response to the EU POPs Regulation. Textile & Leather Review. 2025; 8:961-983. https://doi.org/10.31881/TLR.2025.961

How to link: https://doi.org/10.31881/TLR.2025.961

Published: 11 December 2025

Degradation Characteristics of PBDEs in Flame-Retardant Textiles in Response to the EU POPs Regulation

Fangzheng YUAN[1*], Hong ZHANG[2]

[1]Henan Zhengda Law Firm, Zhengzhou 450000, Henan, China

[2]School of Law, Guizhou Minzu University, Guiyang 550025, Guizhou, China

*15538125092@163.com

Article
https://doi.org/10.31881/TLR.2025.961
Received 24 July 2025; Accepted 18 September 2025; Published 11 December 2025

ABSTRACT

The EU persistent organic pollutants (POPs) Regulation imposes strict limit requirements on the residues of polybrominated diphenyl ethers (PBDEs) in flame-retardant textiles. However, due to the stable structure and strong fiber matrix shielding effect of high-brominated diphenyl ethers, their degradation rate is slow, making it difficult to meet compliance requirements during their service life. This paper focuses on the migration and degradation characteristics of high-brominated PBDEs under real service conditions, constructs a multi-factor synergistic simulation system integrating ultraviolet (UV) irradiation, wet-heat cycling, and periodic water washing, and uses gas chromatography–mass spectrometry (GC–MS) to quantitatively track polybrominated isomers. The results show that under the synergistic conditions of a triple stress, the concentration of BDE-209 dropped from 8.5 mg/kg to 1.2 mg/kg, and the concentrations of the main products BDE-153 and BDE-99 were 3.2 mg/kg and 2.9 mg/kg, respectively. The results indicate that this method effectively promotes debromination and contributes to the control of residues within the EU POPs thresholds applicable to textile products. Although the total PBDE concentration remains within the EU POPs thresholds applicable to textile categories, these products exhibit persistence, bioaccumulation potential, and adverse biological effects that are comparable to or higher than that of the parent compound. This highlights that regulatory compliance should be evaluated together with the inherent toxicity of degradation products to provide a more comprehensive assessment of environmental safety.

KEYWORDS

flame retardant textiles, polybrominated diphenyl ethers, environmental degradation pathway, POPs regulation, kinetic modeling

INTRODUCTION

Flame-retardant textiles are widely used in transportation, construction, and home furnishings, and their flame-retardant properties are crucial to personal safety. Polybrominated diphenyl ether flame retardants are widely used in fabric finishing due to their thermal stability and durability [1,2]. However, polybrominated diphenyl ethers (PBDEs) have been listed as restricted substances in the EU persistent

organic pollutants (POPs) Regulation, and the limit values have become increasingly stringent. According to the amendments of Regulation (EU) 2019/1021, the sum of tetra-, penta-, hexa-, hepta-, and deca-BDE in mixtures or articles is restricted to 10 mg/kg. For articles containing recovered materials, the permissible level will be reduced from 500 mg/kg to 350 mg/kg by December 2025, and further to 200 mg/kg by December 2027. For toys and childcare articles made of recovered materials, the concentration must not exceed 10 mg/kg within 18 months after entry into force. These differentiated thresholds and staged transition periods indicate that compliance assessment should not be reduced to a single numerical limit, but must be understood within a multi-level regulatory framework. The residual concentration during the service life has therefore become a critical parameter in evaluating both regulatory compliance and environmental impact [3,4].

Currently, the migration and degradation laws of PBDEs in textiles remain unclear due to their high bromine content, difficulty in release, and limited influence from environmental factors. Under the superposition of stresses such as ultraviolet (UV) radiation, wet heat, and washing, they exhibit heterogeneous, nonlinear, and multi-path behaviors within the fiber [5,6]. Existing studies mostly use static or single-factor conditions, which makes it difficult to reveal their transformation characteristics and degradation rates under real service environments, and lack quantitative analysis of the responses of different isomers [7,8]. Most of these results remain limited by the absence of coupled stress conditions that dominate real service environments, and the toxicological relevance of the degradation intermediates has not been sufficiently addressed. These shortcomings restrict the accuracy of predicting long-term persistence and potential risks of PBDEs in textiles. This study establishes a multi-stress collaborative framework combining UV irradiation, wet-heat cycling, and washing forces, which links the observed debromination pathways with kinetic modeling and toxicological interpretation to provide a more representative assessment of service-related transformations.

Some studies have investigated the migration and degradation characteristics of PBDEs through accelerated aging or static water washing. In contrast, others have monitored changes in isomers using pyrolysis-chromatography and fitted the concentration trend to analyze the debromination behavior [9,10]. However, most of them ignore multi-stress coupling, lack systematic tracking of degradation products, and the relationship between degradation rate and toxic products remains unclear. Compliance remains challenging to ensure [11,12].

To solve the above problems, this paper constructed a multi-stress collaborative simulation platform of UV, wet heat, and washing, combined solid phase extraction and GC-MS quantitative detection, tracks the degradation path and structural evolution of PBDEs, extracts kinetic parameters based on the pseudo-first-order model, and analyzes the dynamic change process inside the fiber. The research focuses on limit control and aims to establish an effective connection between the degradation path and regulatory compliance.

RELATED WORK

The existence state and degradation behavior of PBDEs in flame-retardant textiles have always been the core issues in environmental behavior research. The porous structure of fibers and the wettability of interfaces form a shielding effect, significantly inhibiting migration and delaying degradation. Oumeddour et al. [13] conducted an UV irradiation experiment combined with multiple analytical methods. They found that the degradation rates of decabromodiphenyl ether (DecaBDE) and hexabromocyclododecane (HBCD) exceeded 50%, with the release of volatile products, indicating a risk of migration and release under light conditions [13]. This study shows that high-energy light can trigger the molecular breakage of PBDEs, suggesting potential stability issues during service [13]. Portet Koltalo et al. [14] employed microwave extraction in conjunction with X-ray fluorescence technology to determine the levels of PBDEs in hard plastics. Although there are differences in the migration patterns compared to textile fibers, their analysis of rapid screening errors provides a reference for methodological comparison. This finding reveals that bromine elements and flame retardants do not have a direct correspondence in complex matrices, reflecting the limitations of analytical techniques. Marti et al. [15] compared brominated and halogen-free flame-retardant cotton fabrics and found that halogen-free residues were more stable and did not penetrate the skin, indicating better safety. Although the above studies involve degradation and alternative paths, there is a lack of systematic tracking of PBDEs' behavior under multiple stresses in the fabric system [16,17]. Many of the reported approaches rely on isolated laboratory conditions and describe concentration variations without connecting the observed kinetics to toxicological outcomes or compliance frameworks. The absence of such integration reduces their applicability for evaluating environmental safety. The present work combines degradation kinetics with analysis of toxic product accumulation to address this gap within a textile-specific context.

The photothermal degradation mechanism of PBDEs in polymers and environmental media is crucial for understanding the evolution of their toxicity. Wang et al. [18] analyzed the thermal decomposition pathway of BDE-209 based on density functional theory and noted that it generates toxic products through ether bond cleavage and debromination. This study provides molecular-level evidence in support of the high-temperature treatment mechanism [18]. Sun et al. [19] summarized the toxicity effects and transformation mechanisms of BDE-209 from the perspective of environmental exposure and proposed photothermal degradation control strategies. Most existing experiments are single-stress, lacking the exploration of degradation mechanisms under the combined effects of UV, wet heat, and water washing. Valenti-Quiroga et al. [20] investigated the photolysis reaction of PBDEs in the aqueous phase, revealing the influence of wavelength and water quality on the degradation rate. Although research has expanded the understanding of the photothermal degradation of PBDEs, the kinetic evolution under multiple stresses in solid-state fabrics still lacks systematic verification. Unlike studies confined to single photolytic or thermal

processes, the approach adopted here considers UV irradiation, heat, and washing as concurrent drivers of degradation. This enables clarification of how stress interactions determine both the rate and direction of debromination, while also linking the identified pathways to the toxicological relevance of dominant intermediates, thereby extending current understanding of PBDE transformation in fiber systems.

MATERIALS AND METHODS

Material Preparation

Three typical flame-retardant textiles (polyester-based, cotton-based, and nylon-based) with significant structural differences were selected to cover the common fiber configuration differences. The samples were cut, numbered, and stored in a sealed container for subsequent analysis. Samples were cryo-ground and sieved to avoid thermal degradation.

The initial concentration of PBDEs was determined by solid phase extraction combined with gas chromatography–mass spectrometry (GC–MS) analysis. The target compounds were extracted multiple times with chloroform/n-hexane (1:1) under ultrasonic conditions for pretreatment and then concentrated by nitrogen blowing and purified using a silica gel column to remove impurities. BDE-209, BDE-153, BDE-99, and BDE-47 were quantitatively calibrated separately. Each sample set was injected three times, and the concentration was corrected based on the spiked recovery rate.

To clarify the distribution state of PBDEs in the fibers, the fiber cross-sections were characterized using scanning electron microscopy (SEM) combined with energy-dispersive X-ray spectroscopy (EDS). The results showed that PBDEs were concentrated in the core of nylon, tended to accumulate at the edges of polyester, and were evenly distributed in cotton fibers, providing a structural basis for subsequent migration-factor calculations and degradation pathway modeling.

When the degradation kinetic model was applied, the initial concentration of each sample was used as the boundary condition of the pseudo-first-order reaction rate equation, and its mathematical expression was given as:

$$C(t)=C_0e^{-kt} \quad (1)$$

In formula (1), $C(t)$ is the concentration of PBDEs at any time point; C_0 is the initial concentration; and k is the degradation rate constant. To ensure the accuracy of the model boundary conditions, Table 1 lists the initial total concentration of PBDEs and the proportion distribution of the main isomers in the three types of fiber samples, providing basic data support for subsequent kinetic parameter fitting and analysis of migration behavior.

Table 1 Distribution of initial PBDEs total concentration and isomer ratio of three types of fiber samples

Fiber Type	Total PBDEs concentration (mg/kg)	BDE-209 (%)	BDE-153 (%)	BDE-99 (%)	BDE-47 (%)
Polyester	12.8	72.5	14.3	9.2	4
Cotton	10.4	48.6	22.5	18.3	10.6
Nylon	13.6	80.1	10.2	6.8	2.9

The application of the pseudo-first-order kinetic model in this study is based on the observation that the primary debromination of PBDEs follows a dominant rate-limiting pathway under controlled stress conditions. Although the degradation of high-brominated congeners in textiles involves heterogeneous environments and concurrent migration processes, the exponential decay form of the model adequately captures the overall temporal trend of concentration decline. The high correlation coefficients derived from curve fitting indicate that the model provides an accurate representation of the experimental data within the treatment timescales considered. At the same time, the rate constants derived from this approach should be regarded as effective kinetic parameters that integrate the influence of diffusion resistance and partial secondary reactions, rather than intrinsic reaction constants of a single molecular pathway. This interpretation allows the model to provide a consistent quantitative framework for comparing degradation behaviors under different stress combinations, while acknowledging that more complex mechanisms may operate at the molecular level.

Considering the regulatory effect of different fiber types on the diffusion path, the migration-degradation coupling model expression was further applied:

$$\frac{dC}{dt}=-kC+D\nabla^2 C \quad (2)$$

In formula (2), D is the effective diffusion coefficient of PBDEs in the fiber, and $\nabla^2 C$ is the Laplace operator of the spatial concentration gradient.

Multi-Stress Coupling Experimental Design

To simulate the environmental exposure process of flame-retardant textiles during their actual service life, a collaborative experimental system was constructed to induce continuous superposition degradation through four types of stresses: UV radiation, humidity, heat cycles, and periodic water washing. The simulation system consists of three parts: an UV aging chamber, a constant temperature, humidity, and heat chamber, and a water washing simulation device. A programmable control method is used to ensure the cyclic stability and coupling controllability of each stress condition.

In the UV aging process, UV light in the 280–320 nm band was applied with an average irradiance of 4.5 mW/cm² at the sample surface. The samples were laid out in the light source area to ensure uniform

irradiation. The irradiation energy flux and PBDEs degradation rate were fitted using a pseudo-first-order model, and the irradiation response factor was applied to quantify the light reaction intensity.

Figure 1 shows the UV device and light source layout. In the schematic, the UV lamp array is positioned at the upper section of the irradiation chamber, and the sensor modules are distributed around the exposure area to monitor light intensity in real time. The samples are fixed on separate holders arranged in parallel planes at the center of the chamber to ensure uniform exposure. Product A represents the polyester-based textile, Sample B corresponds to the cotton-based textile, and Sample C corresponds to the nylon-based textile. Their relative positions are indicated to reflect the experimental grouping and to maintain comparability across different fiber types. Arrows in the schematic indicate the propagation direction of UV irradiation and its intersection with each sample position, while the sensor connection lines illustrate the link between the monitoring points and the data listed in Table 2. By placing irradiation sensor arrays at different positions within the sample layer, the light intensity data for each measuring point was recorded. The irradiance mean and standard deviation results for typical measuring points are listed in Table 2. The numerical values show that the coefficient of variation of the irradiance distribution in the entire effective area is controlled within the acceptable error range.

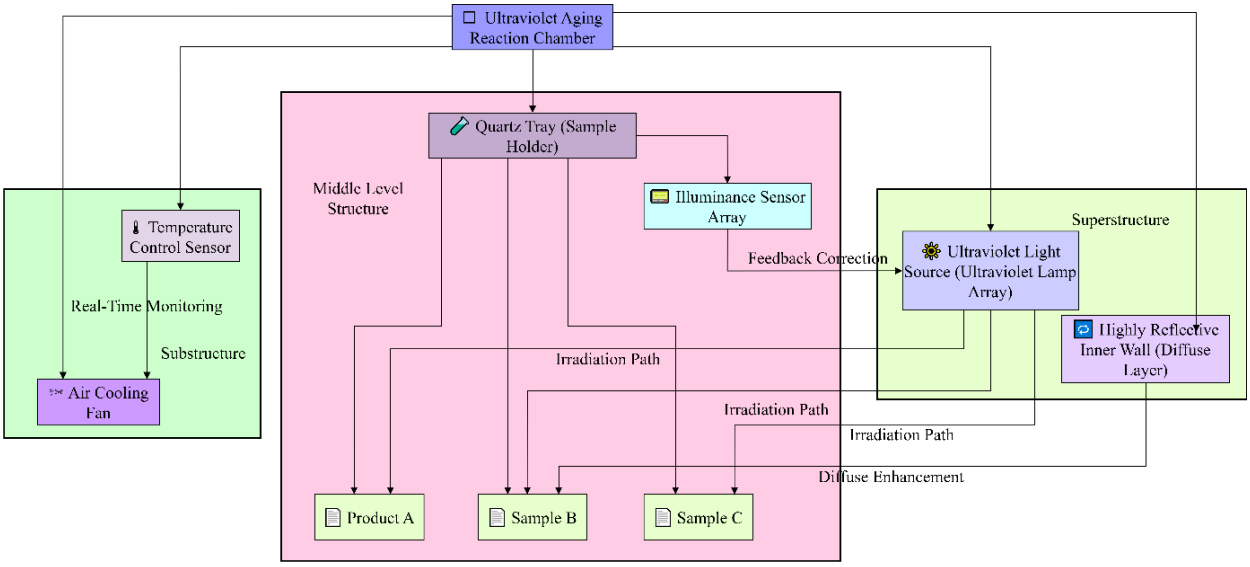

Figure 1. Schematic diagram of the cross-sectional structure and light source distribution of the UV aging experimental device

Table 2. Statistics of the mean and standard deviation of irradiance at different measuring points on the sample irradiation plane

Sensor Position	Mean Irradiance (mW/cm²)	Standard Deviation (mW/cm²)	Coefficient of Variation (%)
Center	4.52	0.08	1.77
Front-Left	4.48	0.11	2.46
Front-Right	4.54	0.09	1.98
Rear-Left	4.47	0.13	2.91

Rear-Right	4.5	0.1	2.22
Average	4.5	0.1	2.27

The wet heat treatment was conducted at 75°C and 85% relative humidity, with four stages: heating, constant temperature, cooling, and drying, resulting in a cyclic change that strengthened the sample's response to alternating temperature and humidity stress. The samples were tensioned and fixed on a high-permeability bracket. The system features an embedded temperature and humidity feedback sensor, which adjusts parameters in real-time and records the fiber's moisture content and deformation coefficient to characterize the synergistic effect of heat-induced deconstruction and moisture polarity migration. The UV source operated in the 280–320 nm range with a spectral peak at approximately 305 nm and a half bandwidth of about 40 nm. Over each 20 h irradiation cycle, the cumulative dose on the sample surface was calculated to be 3.24×10^6 J/m², providing a consistent basis for dose–response evaluation.

The water washing simulation utilized a program-controlled system that complied with ISO 6330. The temperature was set at 50 °C, a low-foaming surfactant system was employed, and each round of washing was completed under constant shear conditions. Freeze-drying was then performed to prevent further thermal migration. The shear induced diffusion model was applied to evaluate the release response of PBDEs.

The three types of stress were analyzed in a unified treatment stage, with each stage corresponding to 20 h of irradiation, one wet-heat cycle, and two water-washing operations to ensure the consistency and comparability among the experimental paths. Through multi-cycle composite treatment, the concentration changes and debromination pathways of the main PBDE isomers were systematically tracked, and a coupled evaluation system integrating degradation and migration was ultimately constructed.

PBDEs Extraction and Purification

After the service simulation treatment, the samples were pre-cooled, sealed, and numbered, and were pre-homogenized under constant temperature conditions to preserve the original state of PBDEs and their degradation products. After the samples were split according to the mass standard, the target compounds were extracted in chloroform/n-hexane (1:1) by an ultrasound-assisted method, and the isomers were extracted by combining ultrasonication and temperature control.

After centrifugation and dehydration, the extract was transferred to the solid-phase extraction system, and the co-extracts were stripped by gradient elution using a macroporous silica column to ensure consistency in the retention rate and migration path of the PBDEs.

Figure 2 shows the differences in chromatographic responses of the components in each segment of the eluent under different polarity gradients. It can be observed that there is a significant difference in

retention time between the main component and the degradation product, which provides a basis for subsequent quantitative analysis.

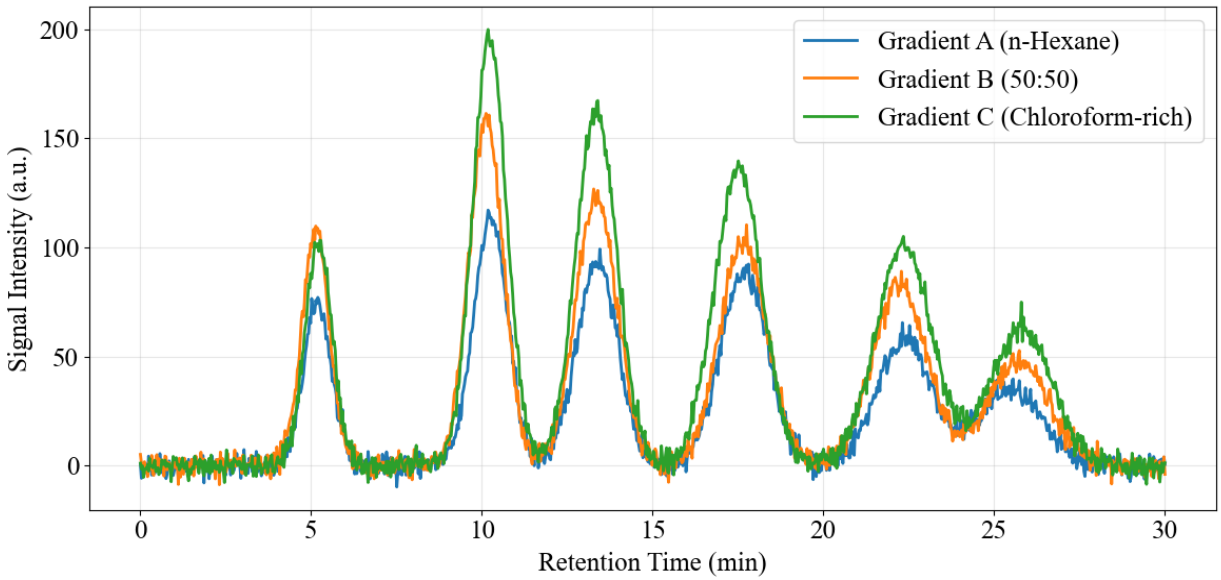

Figure 2. Chromatograms of components after PBDEs extraction and purification

During the purification process, a dual-channel separation strategy was employed to simultaneously process the high-bromine parent and the low-bromine product, thereby avoiding chromatographic overlap. To verify the retention efficiency of the purification process, internal standard calibration was applied, and the recovery rate of each stage was evaluated using the standard curve method. To ensure the conservation of substances and quality consistency during the extraction and purification process, the system efficiency factor η is defined as:

$$\eta = \frac{C_{meas} \cdot V_{final}}{C_{init} \cdot m_{sample}} \quad (3)$$

In formula (3), C_{meas} is the PBDEs concentration measured in the final sample; V_{final} is the volume of the concentrated solution; C_{init} is the initial PBDEs concentration of the fiber; and m_{sample} is the mass of the treated sample.

GC-MS Quantitative Analysis

The test solution was directly injected after purification and concentration, and PBDEs and their degradation products were quantitatively detected using a GC-MS instrument. Split injection and a fused-silica capillary column were utilized for high-resolution separations, and the heating program was optimized to prevent tailing of high-boiling components. Each component was separated according to the

number of bromine atoms and spatial configuration to ensure that the response signals of BDE-209, BDE-153, BDE-99, and BDE-47 did not overlap.

The concentration calibration adopted the five-point external standard method to construct a standard curve for regressing the concentration of each isomer. The fitting function was as follows:

$$A_i = k_i \cdot C_i + b_i \quad (4)$$

In formula (4), A_i represents the chromatographic peak area of the i-th PBDEs isomer; C_i is the corresponding concentration; k_i is the response coefficient; and b_i is the baseline drift correction constant.

The scanning and selected ion monitoring (SIM) modes were combined to improve substance identification and specificity. The SIM channels were set with characteristic ion pairs for each isomer, and the abundance ratio window was optimized to reduce co-extraction interference. The peak area integration method was used for data processing, combining retention time and ion abundance to identify the target component.

Method validation was performed to confirm the reliability of PBDE quantification. Table 3 summarizes the quality assurance parameters, including detection limits, quantification limits, spiked recovery, repeatability of parallel samples, and blank results. The values demonstrate sufficient sensitivity and accuracy to support the concentration differences observed in this study.

Table 3. Quality assurance parameters for PBDEs analysis

Analyte	LOD (mg/kg)	LOQ (mg/kg)	Spiked recovery (%)	RSD of parallel samples (%)	Blank result
BDE-209	0.02	0.05	89–104	6.5	Not detected
BDE-153	0.01	0.03	92–107	5.8	Not detected
BDE-99	0.01	0.03	85–102	7.2	Not detected
BDE-47	0.01	0.03	90–108	6.1	Not detected

As shown in Table 3, the LOD and LOQ values for the target congeners were below 0.05 mg/kg, indicating sufficient sensitivity for detecting low-level residues in textiles. The spiked recovery rates ranged from 85% to 108%, which falls within the acceptable range for quantitative analysis and demonstrates satisfactory accuracy. The relative standard deviations of parallel samples were all below 8%, confirming good repeatability of the measurements. Both process and vessel blanks showed non-detectable levels, excluding any background interference. These results confirm that the analytical method provides reliable support for the concentration differences reported in this study.

Construction of Coupled Kinetic Model of Degradation and Migration

To comprehensively describe the changes in the spatiotemporal behavior of PBDEs under multiple stresses, a coupled kinetic model integrating degradation and migration processes was developed. Taking BDE-209 as the main target, combined with the concentration change sequence of its main degradation products BDE-153, BDE-99, and BDE-47, a pseudo-first-order kinetic equation was constructed based on the measured data, and the time evolution law of PBDEs residues normalized by sample mass $C(t)$ was used to describe it:

$$C(t)=C_0 \cdot e^{-kt} \tag{5}$$

In formula (5), C_0 is the initial concentration, k is the degradation rate constant, and t is the treatment time in hours. The least squares method was used to perform nonlinear regression on the measured data, extract the k value under each set of conditions, and test the residual sum of squares and determination coefficient of the fitting curve to verify the model fit.

During the sample processing, the fiber matrix has a significant retention effect on PBDEs, and some degradation pathways show secondary reaction characteristics. To capture nonlinear changes, the instantaneous degradation rate function was applied:

$$\frac{dC}{dt}=-k \cdot C(t) \tag{6}$$

The discrete derivative sequence was constructed using the concentration difference method, and the slope of the fitting curve was differentially analyzed to identify the dynamic deviation trend of the degradation rate concerning the treatment stage.

To further remove the interference of migration effects on the degradation path, the theoretical correction concentration $C_{corr}(t)$ was applied:

$$C_{corr}(t)=C(t)+M(t) \tag{7}$$

In formula (7), $M(t)$ represents the cumulative amount of PBDEs that migrated to the surface or are lost due to washing. This corrected concentration was used as the basis for kinetic modeling and the corrected rate constants were recalculated. The cumulative migration term $M(t)$ was determined by preparing cross-sectional slices of the treated fibers, quantifying PBDEs in each layer, and integrating the amounts along the thickness direction. The cumulative migrated load was normalized by sample mass, and the

resulting values were fitted to the migration–degradation coupled model to obtain the migration rate constant km through nonlinear regression of *M(t)* as a function of treatment time.

To characterize the structural dependence between products, the relative reaction factor R_f is defined as:

$$R_f = \frac{k_i}{k_{209}} \tag{8}$$

In formula (8), k_i is the rate constant of the degradation product BDE-153, BDE-99 or BDE-47, and k_{209} is the degradation rate of the parent BDE-209.

At the same time, to analyze the migration behavior of PBDEs within the fiber, the longitudinal profile concentration gradient method was employed to sample the treated specimens in the thickness direction and construct a spatial distribution profile. The migration load per unit area Q_x expression is:

$$Q_x = \frac{1}{\Delta x}\int_x^{x+\Delta x} C(x')dx' \tag{9}$$

In formula (9), $C(x')$ is the concentration of PBDEs at position x', and Δx is the sample layer thickness interval.

To quantitatively characterize the migration ability of PBDEs from the interior to the surface, the migration factor MF is defined:

$$MF = \frac{C_s}{C_t} \tag{10}$$

In formula (10), C_s is the concentration of PBDEs in the surface area, and C_t is the average concentration of the entire sample.

Combining the GC-MS test results with the concentration data of the imbalanced area of the profile, the degradation and migration synergy coefficient χ is defined as:

$$\chi = \frac{M_d}{M_d + M_m} \tag{11}$$

In formula (11), M_d is the reduction of PBDEs due to degradation, and M_m is the loss due to migration.

Based on the comprehensive consideration of the two behaviors, a degradation-migration joint kinetic model was constructed:

$$C(t) = C_0 \cdot e^{-(k+k_m)t} \tag{12}$$

In formula (12), k_m is the migration rate constant, which is extracted by model regression. The ratio k_m/k can be used to quantitatively evaluate the relative contribution of migration to the overall removal of PBDEs.

EXPERIMENTAL RESULTS

Degradation Characteristics of PBDEs under Synergistic Effects of Multiple Stresses

In the flame-retardant textile PBDEs degradation experiment, the migration and transformation characteristics of BDE-209 and its main degradation products BDE-153, BDE-99, and BDE-47 were systematically analyzed by simulating different stress conditions. BDE-209 has a stable structure and a complex degradation pathway, and is prone to generating debrominated products to varying degrees; BDE-153 and BDE-99 have enhanced mobility and reactivity, while BDE-47 has a higher potential for environmental diffusion. The experiment used single stress (UV S1, moist heat S2, water washing S3), two stress combinations (UV + moist heat S4, UV + water washing S5, moist heat + water washing S6), and a coupled combination of three stresses (S7), and dynamically tracked the degradation effects and synergistic responses under various conditions for 180 hours. The treatment phase variables were used uniformly, and the equivalent time, water washing rounds, and wet heat cycles were integrated to make each path comparable and valuable for analysis. Figure 3 shows the trend of BDE-209 content and the composition of PBDEs products at the end of each experimental group.

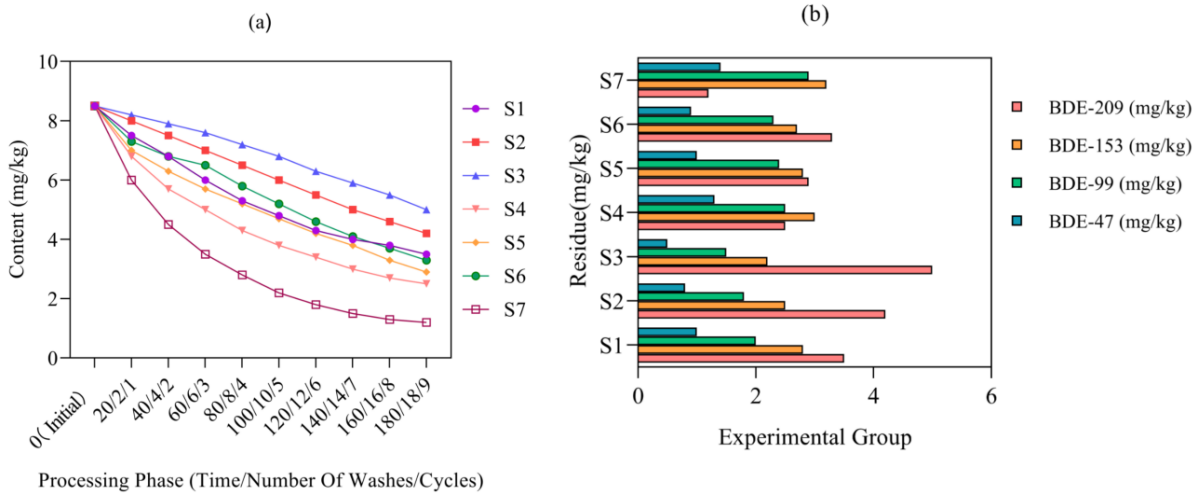

Figure 3. Changes in PBDEs content and final residual distribution. (a) Changes in BDE-209 concentration at each treatment stage, (b) Final composition and total residual content of PBDEs in each group

During the dynamic degradation process, BDE-209 shows a downward trend in all seven treatment paths, and the degradation rate is significantly affected by the stress type and combination mode. In the three-stress coupling group, BDE-209 decreased from 8.5 mg/kg to 1.2 mg/kg, indicating that the combined stresses weaken the fiber shielding effect and enhance molecular reactivity; the endpoint concentrations of the UV+humid heat and UV+water washing groups were 2.5 and 2.9 mg/kg, respectively, indicating that UV light is the main driver; while the residue in the water washing single factor group was still 5.0 mg/kg, indicating that physical disturbance has limited effect on the fracture. In the three-stress group, while BDE-209 was significantly degraded, the concentrations of BDE-153, BDE-99, and BDE-47 were 3.2, 2.9, and 1.4 mg/kg, respectively, resulting in a total residue of 8.7 mg/kg, which remains below the EU POPs threshold applicable to textiles. In the UV + wet heat group, although BDE-209 was reduced to 2.5 mg/kg, the product accumulated to 6.8 mg/kg, and the total load reached 9.3 mg/kg, indicating that some intermediates are stable, limiting further decomposition. In the UV group, BDE-153 was 2.8 mg/kg and BDE-47 was only 1.0 mg/kg, indicating that although light can stimulate the reaction, the degradation depth is insufficient. The overall results show that multi-stress synergy not only improves the degradation rate of PBDEs but also has significant advantages in controlling the final residue.

To verify the significance of these differences, statistical analysis was performed, and the results are presented in Table 4. BDE-209, BDE-153, BDE-99, and BDE-47 all exhibited significant differences across stress conditions ($p < 0.001$), with the triple stress group (S7) showing the most pronounced reduction in BDE-209 compared with single-stress treatments.

Table 4. Final concentrations of PBDEs under different stress conditions with statistical analysis (corresponding to Figure 3b).

Stress group	BDE-209 (mg/kg)	BDE-153 (mg/kg)	BDE-99 (mg/kg)	BDE-47 (mg/kg)
S1 (UV)	3.50 ± 0.18	2.80 ± 0.14	2.00 ± 0.10	1.00 ± 0.05
S2 (Heat & Humidity)	4.20 ± 0.21	2.50 ± 0.13	1.80 ± 0.09	0.80 ± 0.04
S3 (Washing)	5.00 ± 0.25	2.20 ± 0.11	1.50 ± 0.08	0.50 ± 0.03
S4 (UV + Heat)	2.50 ± 0.13	3.00 ± 0.15	2.50 ± 0.13	1.30 ± 0.07
S5 (UV + Washing)	2.90 ± 0.15	2.80 ± 0.14	2.40 ± 0.12	1.00 ± 0.05
S6 (Heat + Washing)	3.30 ± 0.17	2.70 ± 0.14	2.30 ± 0.12	0.90 ± 0.05
S7 (UV + Heat + Washing)	1.20 ± 0.06	3.20 ± 0.16	2.90 ± 0.15	1.40 ± 0.07
F-value	42.6	27.8	34.2	21.5
p-value	< 0.001	< 0.001	< 0.001	< 0.001

The synergistic effect observed under multiple stresses can be attributed to the interaction of distinct physicochemical processes. UV irradiation induces photolytic cleavage of ether bonds in BDE-209 and

generates reactive intermediates that trigger debromination. Exposure to heat and humidity alters the fiber microstructure by reducing crystallinity and increasing molecular mobility, which decreases the shielding effect of the matrix and allows deeper penetration of irradiation. Washing imposes hydrodynamic shear and solvation forces that remove loosely bound degradation products from the fiber surface and promote diffusion of PBDEs toward the exterior. When combined, these stresses weaken the protective barrier of the fiber, increase accessibility of reactive sites, and prevent product accumulation, resulting in an enhanced degradation efficiency beyond the sum of individual effects.

Structural Distribution Characteristics of Degradation Products

To explore the degradation pathway and product distribution characteristics of PBDEs in flame-retardant textiles, this experiment was designed with multi-stage stress treatment to simulate environmental changes under various service conditions, systematically investigating the migration and degradation behavior of PBDEs. The UV irradiation stage (A1) simulated light aging and broke the stable bonds of high-brominated PBDEs; the wet-heat cycle stage (B2) accelerated the reaction rate through high temperatures and humidity; and the water washing stage (C3) promoted product release through mechanical shearing and solvent action. The chemical analysis focused on debrominated isomers such as BDE-208 and BDE-207, and small-molecule products. GC-MS was used to quantify changes in product abundance under multi-stage stress. Figure 4 shows the dynamic evolution trend of the products at each stage.

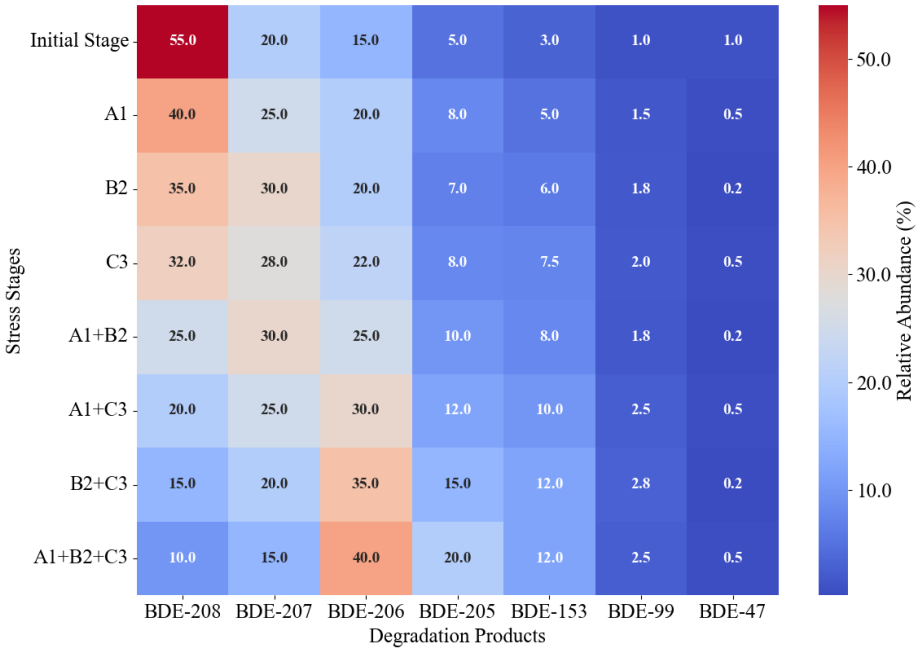

Figure 4. Distribution of PBDEs degradation products in flame retardant fabrics under multi-stage stress treatment

Figure 4 shows that in the initial stage, BDE-208 accounted for 55% and was the main component. After UV irradiation, the proportion of BDE-208 dropped to 40%, while BDE-207 and BDE-206 increased, indicating that photochemical reactions induce debromination of BDE-208. The wet heat cycle further promoted the process, and BDE-208 dropped to 35%. At the same time, BDE-153 and BDE-99 gradually accumulated, indicating that the wet heat environment has a catalytic effect on the debromination process. In the cyclic water washing, the proportion of BDE-206 increased to 22%. Under the three-stress combination, BDE-208 decreased to 10%, and BDE-206 and BDE-205 increased to 40% and 20%, respectively, indicating that the superposition of multiple stresses significantly improves the degradation efficiency. This synergistic effect may be attributed to the weakening of the fiber shielding effect and the superposition of reaction rates, supporting the potential of multi-stage treatment in degrading PBDEs. The observed accumulation of BDE-153 and BDE-99 demonstrates that debromination enhances molecular mobility but does not necessarily reduce toxicological burden. Although the measured levels remain below the regulatory threshold, previous toxicological studies indicate that these congeners present stronger endocrine-disrupting effects and higher bioavailability, suggesting that their environmental implications require systematic consideration in parallel with concentration control. The relative distribution of products reflects stress-dependent pathways of debromination. UV irradiation favors stepwise removal of bromine from para-substituted sites, producing intermediates such as BDE-208 and BDE-207. Wet heat promotes deeper debromination within the fiber matrix, leading to increased formation of medium-brominated congeners. Periodic washing facilitates the appearance of lower-brominated congeners by removing intermediates and sustaining exposure of internal molecules. The detection of BDE-206 and BDE-205 under combined stresses indicates parallel degradation routes, suggesting that multiple scission sites are activated when shielding effects are reduced. These distributions demonstrate that stress-specific interactions determine not only the rate but also the mechanistic direction of PBDE transformation.

Degradation Kinetics Fitting Results

To characterize the temporal variation of the residual concentration of high-brominated PBDEs in flame-retardant textiles under various service conditions, this study conducted accelerated degradation experiments under typical conditions. It employed a pseudo-first-order kinetic model for regression analysis to achieve quantitative fitting. This section complements Section 4.1. The former focuses on the change in residual concentration. At the same time, this section extracts the degradation rate constant and constructs a comparison system to double-verify the kinetic evolution of BDE-209 under simulated conditions. Figure 5 shows the comparison between the measured concentration and the fitting curve, as well as the distribution of degradation rate constants under various conditions.

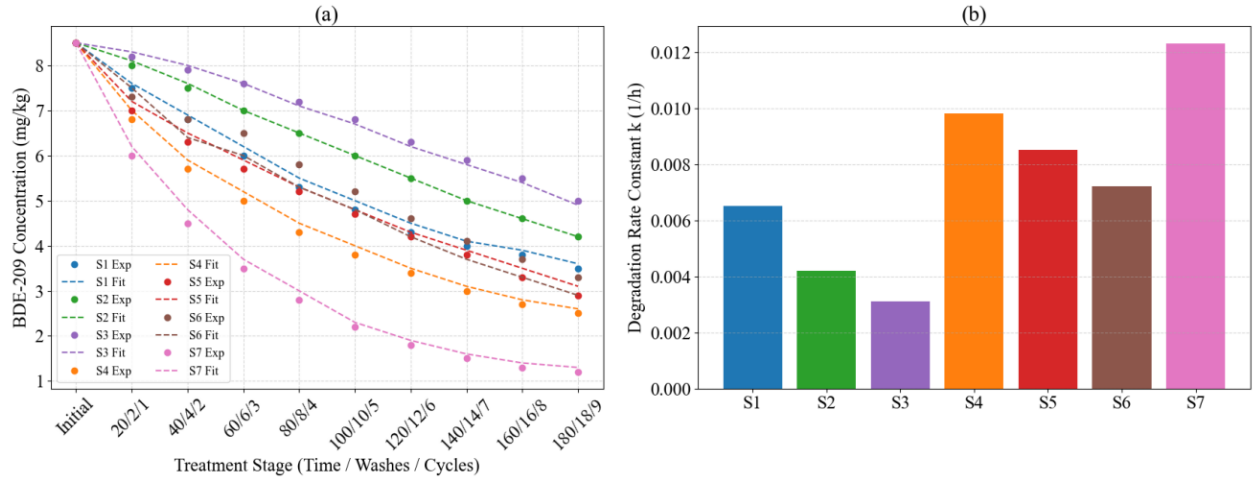

Figure 5. Degradation trend and rate analysis of BDE-209 under multiple stresses. (a) Comparison between measured concentration and fitting curve, (b) Degradation rate constant under various stress conditions

Under single UV stress, the concentration of BDE-209 dropped from 8.5 mg/kg to 3.5 mg/kg, with a fitting rate constant of 0.0065 h^{-1}, and the curve fitting was good. Under wet and hot conditions, the degradation was slow, the residue was higher, and the rate constant dropped to 0.0042 h^{-1}, reflecting that its destructive effect on the molecular structure is weak. The degradation rate of water washing treatment was slightly lower, with a rate constant of 0.0031 h^{-1}, indicating that the embedding stability of PBDEs limits mechanical desorption. Under the synergy of UV and wet heat, the rate constant increased to 0.0098 h^{-1}, indicating that thermal activation enhanced the photodegradation efficiency. In the combined action of UV and water washing, the rate constant was 0.0085 h^{-1}, indicating a synergistic effect between photolysis and interfacial migration. The rate constant for the combination of wet heat and water washing was only 0.0072 h^{-1}, indicating a weak synergistic effect, and degradation primarily occurs through non-photoinduced pathways. The strongest degradation was achieved under the triple stress coupling condition, with the concentration dropping to 1.2 mg/kg after 180 hours, and the rate constant reaching 0.0123 h^{-1}, indicating that multi-field synergy significantly weakens PBDE stability and promotes their migration and degradation. The overall results indicate that a multi-stress environment increases the degradation rate, with UV radiation playing a leading role. The statistical analysis of the degradation rate constants is summarized in Table 5. The observed concentration differences among stress conditions were higher than the quantification limits and were supported by the recovery and repeatability tests, which demonstrates that these variations are analytically reliable. The results indicate that the triple stress condition (S7) produces a significantly higher degradation rate constant than the UV single stress condition (S1) ($p < 0.01$).

Table 5. Degradation rate constants of BDE-209 under different stress conditions with statistical analysis (corresponding to Figure 5b).

Stress group	k (h^{-1})	Significance (vs. UV)
S1 (UV)	0.0065 ± 0.0003	–
S2 (Heat & Humidity)	0.0042 ± 0.0002	* $p < 0.05$
S3 (Washing)	0.0031 ± 0.0002	* $p < 0.05$
S4 (UV + Heat)	0.0098 ± 0.0005	** $p < 0.01$
S5 (UV + Washing)	0.0085 ± 0.0004	** $p < 0.01$
S6 (Heat + Washing)	0.0072 ± 0.0004	* $p < 0.05$
S7 (All conditions)	0.0123 ± 0.0006	** $p < 0.01$

The higher kinetic constants observed under combined stresses are consistent with a cooperative mechanism involving photolytic initiation, thermally assisted bond destabilization, and washing-induced product removal. The wet heat environment reduces the activation energy of bond scission by disrupting bromine-substituted aromatic structures and increases segmental mobility, facilitating diffusion of PBDEs to reactive sites. Washing continuously desorbs intermediate products from the surface, preventing shielding of internal molecules and maintaining photon access. This interplay maintains active photolysis pathways and accounts for the marked increase in degradation rate constants under the triple stress condition.

Regulatory Effect of Fiber Matrix on Degradation-Migration Behavior

To reveal the migration characteristics of highly brominated diphenyl ethers in different fiber matrices, this study systematically measured the concentration profiles of PBDE isomers in the depth direction of fabrics under simulated service conditions. Three typical fibers—cotton, polyester, and nylon—were selected, representing natural fibers, hydrophobic polyester, and dense nylon, respectively. The three fibers differ significantly in molecular polarity, crystallinity, and surface energy. By comparing the profiles of multiple isomers, the enrichment and attenuation of PBDEs from the fiber surface to the inside were analyzed, and the basis for understanding their migration shielding effect was established. Figure 6 shows the depth concentration variation trend of different isomers in the three types of fibers.

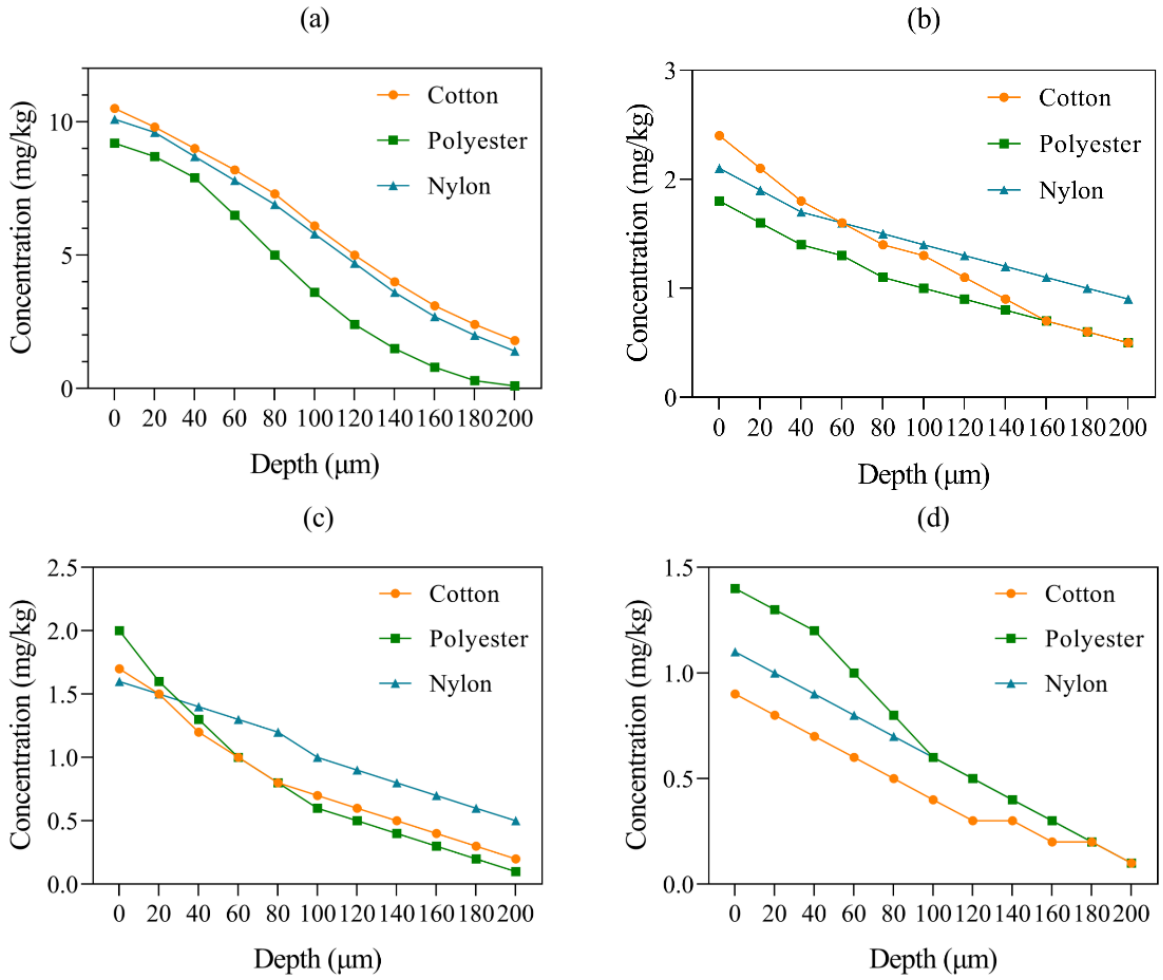

Figure 6. Migration depth profiles of different PBDEs isomers in three fiber materials. (a) BDE-209, (b) BDE-153, (c) BDE-99 (d) BDE-47

In the migration profile of BDE-209, the concentration of cotton fiber decreased from 10.5 mg/kg to 1.8 mg/kg over the range of 0–200 μm, exhibiting a slow attenuation trend from the outside to the inside, which offers little hindrance to the migration of PBDEs. The concentration of polyester on the surface was 9.2 mg/kg, and it decreased to 3.6 mg/kg at 100 μm, indicating that its high crystallinity and hydrophobicity have a significant shielding effect on BDE-209. The nylon curve was between the two, and its migration was significantly affected by the regularity of molecular arrangement. Among the two medium brominated isomers, BDE-153 and BDE-99, the concentrations of the three types of fibers were quite different. For example, BDE-153 in cotton still has 0.5 mg/kg in the deep layer, whereas BDE-99 in polyester is only 0.1 mg/kg, indicating that low-molecular-weight isomers are more likely to be retained in the surface layer of dense polyester, and their mobility is significantly limited. BDE-47, as the lowest brominated product, has the shallowest profile gradient among all types of fibers, indicating that its migration ability is controlled by molecular size and polarity, and it can more easily penetrate the fiber gaps.

In summary, the migration behavior of PBDEs is significantly influenced by the fiber structure, with crystallinity and polarity differences being the primary determining factors. The depth-resolved concentration gradients provided the basis for calculating *M(t)* as the integrated migrated fraction. The temporal evolution of these values was fitted with the coupled model, from which k_m was derived, linking the experimental profiles to the kinetic parameters.

Application and Interpretation of the Migration–Degradation Coupling Model

The migration and degradation of BDE-209 show significant differences in different fiber systems. Cotton fibers, due to their loose structure, facilitate diffusion of the contaminant, while the dense arrangement and hydrophobic properties of polyester fibers restrict migration. In contrast, nylon fibers, due to their polar groups, create a balance between migration and adsorption. To reveal the coupled behavior of PBDEs in fiber matrices, this study introduced a migration-degradation coupling model based on fitted depth distributions. This model splits the overall residual concentration into migration-dominated and degradation-dominated contributions, and further compares the dynamic removal mechanisms of BDE-209 in different fiber materials. Figure 7 shows the fitted depth distribution curve on the left, while the separation of migration and degradation contributions is shown on the right.

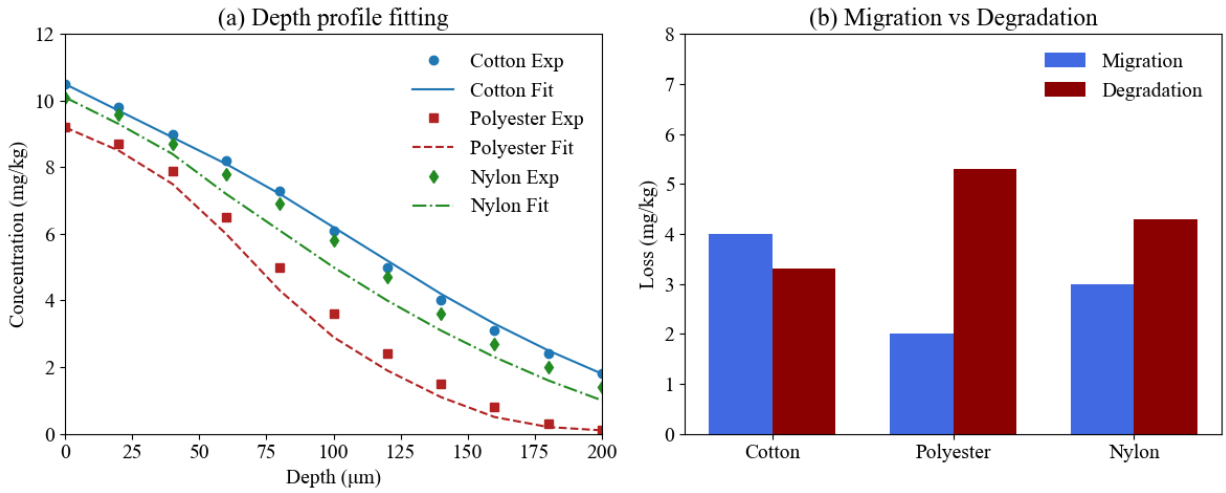

Figure 7. Coupling characteristics of BDE-209 migration and degradation in different fiber materials. (a) Concentration distribution fitting of BDE-209 in the fiber depth direction. (b) Separation analysis of migration and degradation contributions.

The results show that within the depth range of 0–160 μm, the residue level in the surface region of cotton fibers rapidly decreased from 10.5 mg/kg to 3.1 mg/kg, indicating that migration dominates and that open interfiber gaps enhance the combined effects of degradation and migration. Polyester concentrations dropped to 3.6 mg/kg at 100 μm, but migration accounted for less than 30% of total removal, indicating that the high-density structure enhances shielding and increases the contribution of degradation to overall

removal. Nylon retained a residual level of 4.7 mg/kg at 120 μm, demonstrating a dual control mechanism: polarity enhances PBDE binding to the fiber, slowing migration, while some adsorption sites provide stable pathways for degradation. These differences suggest that the fiber matrix structure directly determines the coupled migration-degradation pattern of PBDEs, with cotton exhibiting a migration-dominant pattern, polyester a degradation-dominant pattern, and nylon a balance between migration and degradation.

CONCLUSION

Based on the multi-stress simulation platform, this study constructed a coupling system of UV irradiation, wet heat, and water washing, and combined GC-MS with a pseudo-first-order kinetic model to analyze the degradation and migration characteristics of PBDEs in flame-retardant textiles. Under triple stress, the concentration of BDE-209 decreased from 8.5 mg/kg to 1.2 mg/kg, and the degradation rate constant increased to 0.0123 h^{-1}, which was significantly higher than under single-stress conditions, demonstrating the effectiveness of multi-stress synergy in weakening the fiber shielding effect and accelerating molecular dissociation. The endpoint concentrations of BDE-153 and BDE-99 reached 3.2 mg/kg and 2.9 mg/kg, respectively, reflecting that the debromination chain is more complete and the total residual load remains within the EU POPs thresholds set for textiles.

The distribution of intermediates confirms that distinct debromination pathways are selectively activated under different stresses, and the accelerated removal of PBDEs arises from the interplay of photolytic bond cleavage, thermally induced weakening of the fiber matrix, and hydrodynamic removal of intermediates. The statistical validation presented in Tables 4 and 5 supports the significance of this synergistic effect in both residual concentration and kinetic parameters, reinforcing the robustness of the conclusions.

At the same time, the accumulation of medium-brominated congeners such as BDE-153 and BDE-99 illustrates that the reduction of BDE-209 does not necessarily correspond to a reduction in toxicological risk. These degradation products exhibit persistence and biological relevance that may lead to underestimated hazards if compliance assessment relies solely on concentration thresholds. This highlights the necessity of integrating degradation kinetics with toxicity evaluation to establish a more reliable framework for risk assessment.

The findings provide mechanistic evidence for multi-stress cooperative degradation and offer a quantitative reference for environmentally sustainable textile design. While the selected UV, wet heat, and washing conditions reflect typical service stresses, they represent one accelerated configuration; the quantitative outcomes may differ under other textile matrices or environmental settings. Future work should therefore extend the coupled kinetic–toxicological framework to broader application scenarios, strengthening its role in supporting regulatory compliance and environmental safety assessment.

Author Contributions

Conceptualization – Fangzheng Yuan; methodology – Fangzheng Yuan; investigation – Hong Zhang; resources – Fangzheng Yuan; writing-original draft preparation – Fangzheng Yuan; writing-review and editing – Hong Zhang. All authors have read and agreed to the published version of the manuscript.

Conflicts of Interest

The authors declare no conflict of interest.

Funding

This research received no external funding.

Acknowledgements

Not applicable.

REFERENCES

[1] Olisah C, Melymuk L, Audy O, Kukucka P, Pribylova P, Boudot M. Extremely high levels of PBDEs in children's toys from European markets: Causes and implications for the circular economy. Environmental Sciences Europe. 2024; 36(1):183-194. doi: 10.1186/s12302-024-00999-2

[2] Kajiwara N, Matsukami H, Malarvannan G, Chakraborty P, Covaci A, Takigami H. Recycling plastics containing decabromodiphenyl ether into new consumer products including children's toys purchased in Japan and seventeen other countries. Chemosphere. 2022; 289(1):133179-133207. doi: 10.1016/j.chemosphere.2021.133179

[3] Durak H. Comprehensive assessment of thermochemical processes for sustainable waste management and resource recovery. Processes. 2023; 11(7):2092-2131. doi: 10.3390/pr11072092

[4] Shakil S, Yumna S, Naeem AA. Review of polybrominated diphenyl ethers contamination in environmental compartments of recycling and landfill/dumping facilities: Developed vs. developing regions perspective. International Journal of Environmental Health Research. 2025; 1(1):1-15.

[5] Mokoana VN, Asante JK, Okonkwo OJ. A review on volatilization of flame retarding compounds from polymeric textile materials used in firefighter protective garment. Journal of Fire Sciences. 2023; 41(4):107-121. doi: 10.1177/07349041231171349

[6] Agnihotri S, Sheikh JN. Flame-retardant textile structural composites for construction application: A review. Journal of Materials Science. 2024; 59(5):1788-1818. doi: 10.1007/s10853-023-09312-7

[7] Cantwell C, Song X, Li X, Zhang B. Prediction of adsorption capacity and biodegradability of polybrominated diphenyl ethers in soil. Environmental Science and Pollution Research. 2023; 30(5):12207-12222. doi: 10.1007/s11356-022-22996-9

[8] Wu T, Li Y, Xiao H, Fu M. Molecular modifications and control of processes to facilitate the synergistic degradation of polybrominated diphenyl ethers in soil by plants and microorganisms based on queuing scoring method. Molecules. 2021; 26(13): 3911-3930. doi: 10.3390/molecules26133911

[9] Aldoori H, Bouberka Z, Feuchter H, Khelifi S, Poutch F, Brison L, et al. Recycling of plastics from e-waste via photodegradation in a low-pressure reactor: The case of decabromodiphenyl ether dispersed in poly (acrylonitrile-butadiene-styrene) and poly (carbonate). Molecules. 2023; 28(6):2491-2504. doi: 10.3390/molecules28062491

[10] Benmammar RK, Bouberka Z, Malas C, Carpentier Y, Haider KM, Mundlapati VR, et al. Degradation of Decabromodiphenyl Ether Dispersed in Poly (Acrylo-Butadiene-Styrene) Using a Rotatory Laboratory Pilot Under UV-Visible Irradiation. Molecules. 2024; 29(21):5037-5055. doi: 10.3390/molecules29215037

[11] Smollich E, Merkus V, Klein K, Schmidt T, Sures B. Investigating the photolytic degradation of novel monomeric and polymeric brominated flame retardants: Analytical characterization, acute ecotoxicological effects and influence of sample storage. Environmental Sciences Europe. 2025; 37(1):49-62. doi: 10.1186/s12302-025-01083-z

[12] Hennebert P. The substitution of regulated brominated flame retardants in plastic products and waste and the declared properties of the substitutes in REACH. Detritus. 2021; 16(1):16-25. doi: 10.31025/2611-4135/2021.15122

[13] Oumeddour H, Aldoori H, Bouberka Z, Mundlapati VR, Madhur V, Foissac C, et al. Degradation processes of brominated flame retardants dispersed in high impact polystyrene under UV–visible radiation. Waste Management & Research. 2024; 42(12):1241-1252. doi: 10.1177/0734242X231219626

[14] Portet-Koltalo F, Guibert N, de Mengin-Fondragon F, Frouard A. Evaluation of polybrominated diphenyl ether (PBDE) flame retardants from various materials in professional seating furnishing wastes from French flows. Waste Management. 2021; 131(1):108-116. doi: 10.1016/j.wasman.2021.05.038

[15] Martí M, Alonso C, Manich A, Vilder ID, Coderch L. Flame retardant textile finishing: Thermal analysis and dermal security. Textile Research Journal. 2024; 94(1-2):69-81. doi: 10.1177/00405175231199498

[16] Kaurin T, Pušić T, Dekanić T, Flinčec Grgac S. Impact of washing parameters on thermal characteristics and appearance of proban®—Flame retardant material. Materials. 2022; 15(15):5373-5390. doi: 10.3390/ma15155373

[17] Mazumder N-U-S, Islam MT. Flame retardant finish for textile fibers. Innovative and Emerging Technologies for Textile Dyeing and Finishing. 2021; 1(1):373-405. doi: 10.1002/9781119710288.ch13

[18] Wang Y, Huang J, Wang H, Lan L, Mu X, Xu W, et al. Theoretical study on pyrolysis mechanism of decabromodiphenyl ether (BDE-209) using DFT method. Chemosphere. 2023; 310(1):136904-136919. doi: 10.1016/j.chemosphere.2022.136904

[19] Sun Y, Xu Y, Wu H, Hou J. A critical review on BDE-209: Source, distribution, influencing factors, toxicity, and degradation. Environment International. 2024; 183(1):108410-108431. doi: 10.1016/j.envint.2023.108410

[20] Valentí-Quiroga M, Gonzalez-Olmos R, Auset M, Díaz-Ferrero J. Study of the Photodegradation of PBDEs in Water by UV-LED Technology. Molecules. 2021; 26(14):4229-4247. doi: 10.3390/molecules26144229